

The impact of reorienting cone-beam computed tomographic images in varied head positions on the coordinates of anatomical landmarks

Jae Hun Kim¹, Ho-Gul Jeong^{1,*}, Jae Joon Hwang¹, Jung-Hee Lee¹, Sang-Sun Han^{1,*}

¹Department of Oral and Maxillofacial Radiology, Yonsei University, College of Dentistry, Seoul, Korea

ABSTRACT

Purpose: The aim of this study was to compare the coordinates of anatomical landmarks on cone-beam computed tomographic (CBCT) images in varied head positions before and after reorientation using image analysis software.

Materials and Methods: CBCT images were taken in a normal position and four varied head positions using a dry skull marked with 3 points where gutta percha was fixed. In each of the five radiographic images, reference points were set, 20 anatomical landmarks were identified, and each set of coordinates was calculated. Coordinates in the images from the normally positioned head were compared with those in the images obtained from varied head positions using statistical methods. Post-reorientation coordinates calculated using a three-dimensional image analysis program were also compared to the reference coordinates.

Results: In the original images, statistically significant differences were found between coordinates in the normal-position and varied-position images. However, post-reorientation, no statistically significant differences were found between coordinates in the normal-position and varied-position images.

Conclusion: The changes in head position impacted the coordinates of the anatomical landmarks in three-dimensional images. However, reorientation using image analysis software allowed accurate superimposition onto the reference positions. (*Imaging Sci Dent* 2016; 46: 133-39)

KEY WORDS: Cone-Beam Computed Tomography; Anatomic Landmarks; Orthodontics

Introduction

In recent years, interest in accurate orthodontic treatment planning using three-dimensional imaging technology has increased.^{1,2} The initial three-dimensional computed tomography (CT) techniques, single-detector CT and multi-detector CT, exposed patients to high doses of radiation.³⁻⁸ Recently, the introduction of cone-beam computed tomography (CBCT) has provided an alternative imaging modality with higher resolution, lower cost, and

lower radiation exposure, which has further fueled research into three-dimensional image analysis.^{1,9-13} However, since CBCT images are obtained when the patient is in a sitting position with their head supported by an unreliable head-holding apparatus, unlike traditional forms of CT, it is difficult to replicate head positions in CBCT, potentially hindering accurate comparisons of the results of orthodontic treatment or surgery. Few studies have evaluated the potential effects of low repeatability in images due to variations in head position.^{14,15}

With recent increases in CBCT usage, it has become more common to utilize image analysis programs to process the large amounts of image data created. Some programs provide the ability to adjust the reference plane typically used in CBCT, and this function can be used to compensate for possible image discrepancies when comparing images with different head positions.¹⁶⁻¹⁸ Studies exploring image analysis functionality have reported no

*This study was supported by a new faculty research seed money grant from Yonsei University College of Dentistry (2015-32-0048).

Received January 28, 2016; Revised February 15, 2016; Accepted March 12, 2016

*Correspondence to : Prof. Sang-Sun Han

Department of Oral and Maxillofacial Radiology, Yonsei University, College of Dentistry, 50-1 Yonsei-ro, Seodaemun-gu, Seoul 03722, Korea

(Tel) 82-2-2228-3122, Fax) 82-2-363-5232, E-mail) sshan@yuhs.ac

Prof. Ho-Gul Jeong

Department of Oral and Maxillofacial Radiology, Yonsei University, College of Dentistry, 50-1 Yonsei-ro, Seodaemun-gu, Seoul 03722, Korea

(Tel) 82-2-2228-3124, Fax) 82-2-363-5232, E-mail) rari98@yuhs.ac

discrepancies in length or angle when various head positions were compared to normal-position images.^{1,3,14,16,19,21} However, while image length and angle may not vary according to head positions, coordinates may do so. No previous studies have investigated discrepancies in coordinates. This study aimed to investigate the effects of various head positions on three-dimensional image coordinates and in turn on orthodontic landmarks using a three-dimensional image analysis program.

Materials and Methods

One dry skull was used in this study. In order to simulate the anatomic relationship of the temporomandibular area, base plate wax 1.0 mm in thickness was used to connect the temporal fossa and condylar process. The dry skull was then placed on a tripod for angle adjustment (Fig. 1). Reference coordinates to use in the image analysis

program for superimposition were marked at 3 places on the dry skull using gutta percha.

Three planes from the normal position of the dry skull



Fig. 1. A dry skull fixed to the tripod for cone-beam computed tomography.

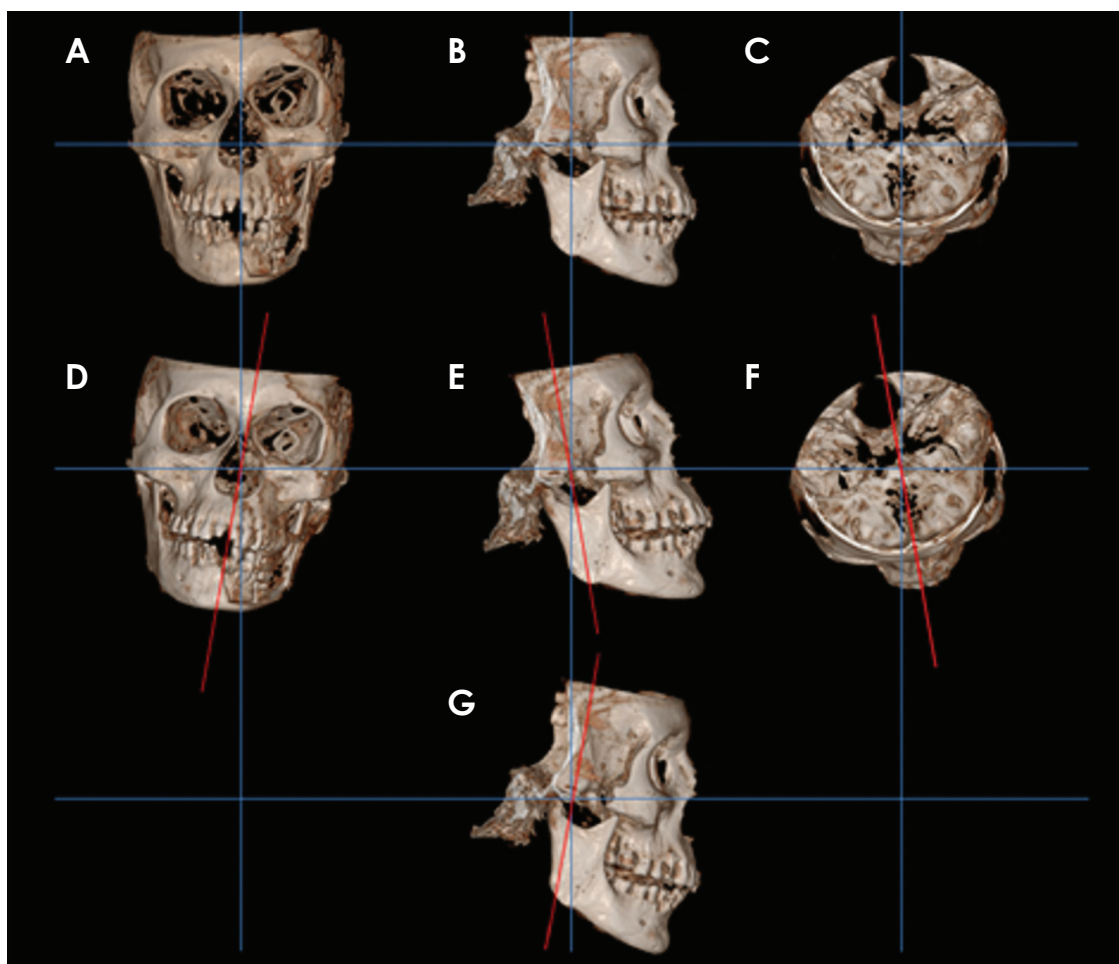


Fig. 2. Three-dimensional cone-beam computed tomography images corresponding to 5 head positions. A. Normal position (horizontal plane). B. Normal position (sagittal plane). C. Normal position (axial plane). D. Five-degree leftward tilting. E. Five-degree extension. F. Five-degree leftward rotation. G. Five-degree flexion.

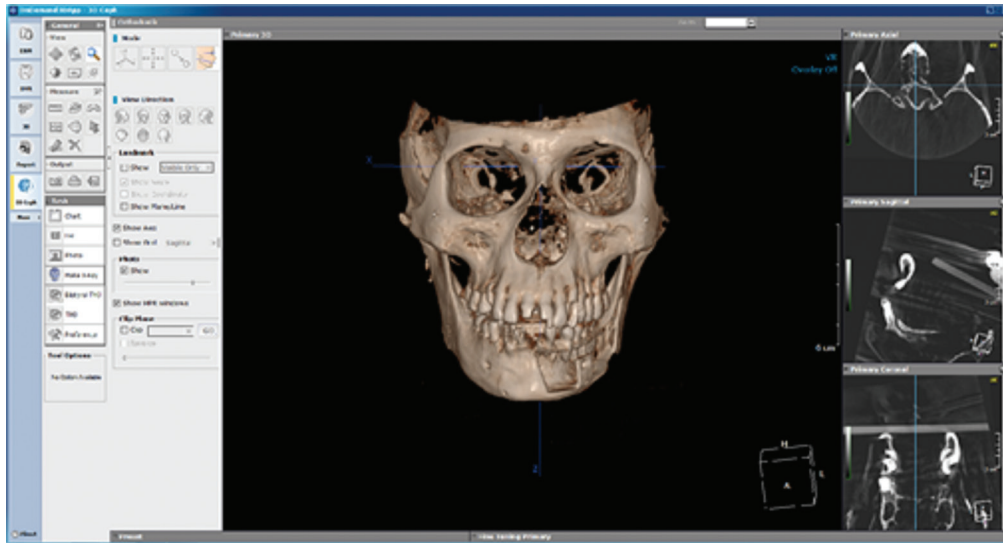


Fig. 3. Reconstructed three-dimensional cone-beam computed tomography images by OnDemand 3D™.

Table 1. Twenty orthodontic landmarks used in this study

Abbreviations	Landmarks	Anatomic region
N	Nasion	Frontonasal suture
A	A point	Premaxilla
B	B point	Anterior surface of the mandibular symphysis
Or-R	Orbitale right	Lateroinferior contour of the right orbit
Or-L	Orbitale left	Lateroinferior contour of the left orbit
Pg	Pogonion	Contour of the bony chin
Me	Menton	Lower border of the mandible
Po-R	Porion right	The most superior lateral point of the right external auditory meatus
Po-L	Porion left	The most superior lateral point of the left external auditory meatus
Co-R	Condyle right	Right condyle
Co-L	Condyle left	Left condyle
UIE-R	Upper incisal edge right	Incisal tip of right upper central incisor
UIE-L	Upper incisal edge left	Incisal tip of right lower central incisor
Go-R	Gonion right	Angle of the right mandibular body
Go-L	Gonion left	Angle of the left mandibular body
S	Sella	Pituitary fossa of the sphenoidal bone
ANS	Anterior nasal spine	Median, sharp bony process of the maxilla
PNS	Posterior nasal spine	Posterior sharp bony process of the maxilla
RP-R	Ramus point right	Posterior border of the right mandibular ramus
RP-L	Ramus point left	Posterior border of the left mandibular ramus

were chosen as references to use when varying head positions. In the study of Togashi et al.,¹⁵ 3 reference planes were defined: the horizontal plane from the left porion to the right orbitale; the sagittal plane crossing the horizontal plane, nasion, and basion; and the longitudinal plane including the right and left porion and crossing the horizontal plane perpendicularly. After the normal position was established, the position of the dry skull was changed through leftward tilting, leftward rotation, extension, and flexion, all in increments of 5° (Fig. 2).

CBCT images were acquired using a RayScan Symphony® apparatus (Ray Co., Hwaseong, Korea) in the Department of Oral and Maxillofacial Radiology, Yonsei University Dental Hospital. The imaging conditions were a tube voltage of 90 kVp, tube current of 10 mA, exposure duration of 19.5 s, and field of view (FOV) of 14 cm × 14 cm. Axial images of 0.38 mm in thickness were reconstructed into three-dimensional images using OnDemand 3D™ (CyberMed Inc., Seoul, Korea) (Fig. 3).

Landmarks conventionally used in orthodontic diagnosis

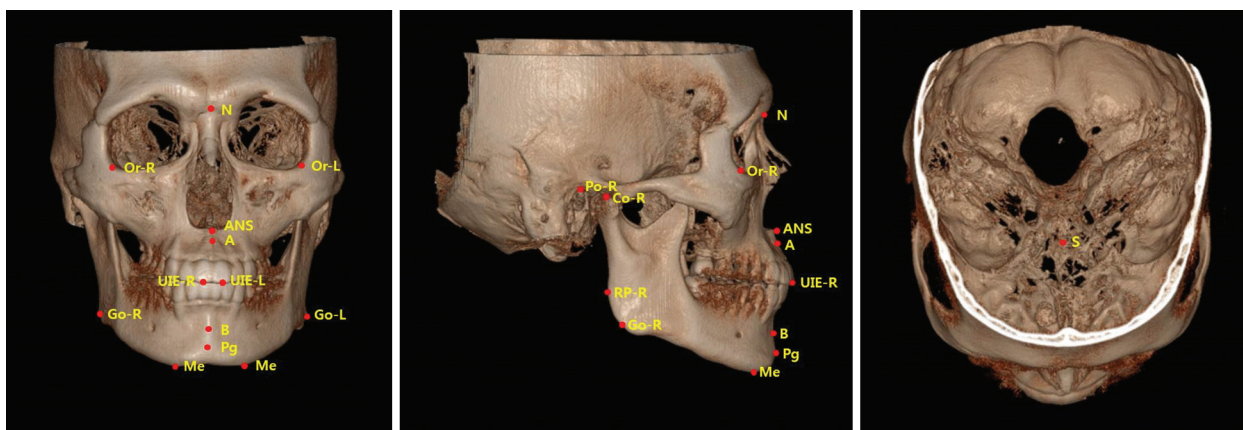


Fig. 4. Twenty landmarks are seen on the reconstructed three-dimensional image.

Table 2. Coordinates before reorientation in 5 head positions

Position	X-coordinate	Y-coordinate	Z-coordinate
Normal	66.35 ± 33.84	54.92 ± 37.15	93.32 ± 31.71
Tilt	74.53 ± 33.22*	59.97 ± 38.10*	100.18 ± 31.69*
Rotation	70.12 ± 33.82	58.40 ± 37.07	87.10 ± 31.62*
Flexion	68.31 ± 33.62*	48.78 ± 37.33*	90.77 ± 31.63*
Extension	66.21 ± 33.26	70.13 ± 35.04*	105.23 ± 30.53*

*: statistically significant difference at $p < 0.05$

or oral surgery were employed (Table 1).²⁰⁻²² Within a span of a week and in two stages, a dentist with OnDemand 3D™ experience took the multiplanar reconstruction of the normal-position and varied-position images, established 20 landmarks, and computed the three-dimensional coordinates (Fig. 4).

The 3D Ceph module of OnDemand 3D™ was used to establish the 3 landmarks fixed with gutta percha to enable the automatic reorientation of the 20 coordinates for superimposition.¹³ This process used the axial plane created by the 3 spots fixed with gutta percha as a platform where the perpendicular sagittal and coronal planes could be established. The computed coordinates obtained in this manner were compared to the post-reorientation coordinates.

In order to evaluate intraobserver agreement, intraclass coefficients were calculated. Agreement in coordinates was compared between the normal-position image and the four varied-position images using the paired t-test for identical landmarks, and p -values < 0.05 were considered to indicate statistical significance. Discrepancies in the coordinates in each landmark among the images were measured as distances. One-way analysis of variance was used to analyze these distances, and Tukey’s post-hoc ana-

Table 3. Distance between normal position and the others in 20 landmarks before reorientation

Landmark	Tilt	Rotation	Flexion	Extension
N	18.84	7.61	9.1	31.06
A	14.8	8.85	9.39	24.09
B	7.27	16.99	8.17	21.66
Or-R	18.16	14.15	16.06	24.11
Or-L	14.44	11.69	10.33	32.73
Pg	9.17	11.4	5.79	19.48
Me	10.28	15.34	4.46	21.05
Po-R	10.48	25.26	6.33	19.68
Po-L	6.71	20.09	6.45	11.31
Co-R	15.37	26.02	7.16	20.74
Co-L	8.49	15.96	6.36	19.52
UIE-R	12.54	20.27	10.41	30.44
UIE-L	20.54	8.86	14.82	27.8
Go-R	12.49	21.42	5.57	13.24
Go-L	18.58	14.27	3.94	16.58
S	11.14	15.47	6.36	22.65
ANS	14.85	10.45	6.59	30.56
PNS	12.15	8.55	5.87	21.73
RP-R	15.97	17.87	7.3	22.9
RP-L	11.14	13.02	7.82	20.57

Mean ± SD 13.17 ± 3.98^b 15.18 ± 5.41^b 7.91 ± 3.11^a 22.59 ± 5.72^c

Same character means a statistically same group (post hoc Tukey’s HSD test, $p > 0.05$)

lysis was employed. The data were analyzed using SPSS version 23.0 (IBM Corp., Armonk, NY, USA).

Results

The landmark coordinates were measured twice and analyzed to determine the intraclass coefficient and showed Cohen’s kappa values greater than 0.8.

The X, Y, and Z coordinates of the normal-position land-

Table 4. Coordinates after reorientation in 5 head positions

Position	X-coordinate	Y-coordinate	Z-coordinate
Normal	-3.66 ± 33.45	-24.14 ± 34.44	19.55 ± 34.75
Tilt	-3.19 ± 33.19	-24.34 ± 35.49	19.40 ± 34.62
Rotation	-3.15 ± 33.62	-23.83 ± 34.28	19.47 ± 34.81
Flexion	-4.01 ± 33.62	-24.41 ± 34.04	19.60 ± 35.14
Extension	-3.71 ± 33.71	-24.08 ± 34.39	19.68 ± 34.50

Table 5. Distance between normal position and the others in 20 landmarks after reorientation

Landmark	Tilt	Rotation	Flexion	Extension
N	0.85	0.8	0.17	0.64
A	0.55	1.47	0.73	1.42
B	10.69	4.08	4.48	5.15
Or-R	3.87	4.78	3.4	1.73
Or-L	5.72	1.43	6.24	4.78
Pg	2.04	1.49	1.38	2.23
Me	1.14	3.26	2.36	0.72
Po-R	0.58	1.79	1.29	1.78
Po-L	3.75	1.53	2.81	2.05
Co-R	1.16	1.08	1.92	0.59
Co-L	1.29	1.03	1.86	0.62
UIE-R	1.87	0.9	0.84	0.88
UIE-L	1.13	1.79	1.2	1.37
Go-R	1.58	0.74	1.7	1.9
Go-L	8.31	0.47	4.86	2.98
S	3.9	0.88	2.26	1.1
ANS	2.68	2.62	0.9	2.58
PNS	0.95	1.77	2.15	0.58
RP-R	0.25	0.95	0.26	0.49
RP-L	0.64	0.52	0.74	0.34
Mean \pm SD	2.65 ± 2.77	1.67 ± 1.17	2.08 ± 1.60	1.70 ± 1.35

marks and the varied-position landmarks are shown in Table 2. Statistically significant differences were associated with five-degree tilting and flexion in the X coordinates, five-degree tilting, flexion, and extension in the Y coordinates, and all of the altered positions in the Z coordinates. The distances between the normal-position coordinates and the corresponding coordinates in the varied-position images were compared to determine the degree of error between the coordinates, and statistically significant differences were found (Table 3). The mean and standard deviation of the distances were 13.17 ± 3.98 mm for tilting, 15.18 ± 5.41 mm for rotation, 7.91 ± 3.11 mm for flexion, and 22.59 ± 5.72 mm for extension. The five-degree flexion image showed the shortest distance, whereas the five-degree extension image showed the greatest distance. In the left-rotation images, the distances obtained for all the right-side landmarks, such as Or, Po, Co, UIE, Go and RP, were longer than the distances obtained for the left-

side landmarks. Similar results were found in the left-tilted images, except for UIE and Go.

The post-reorientation coordinates are shown in Table 4. No statistically significant differences were found between coordinates in the normal-position image and in the four varied-position images (Table 5).

Discussion

Previous studies have found that changing the position of the head does not affect length and angle measurements,^{1,3,14,16,19,21} and likewise, many investigations have attempted to characterize measurement errors in orthodontic diagnoses associated with changing head positions. However, no studies have assessed the degree of error between repeated images taken with slightly different head positions. The protocol involved in obtaining CBCT images does not allow perfectly standardized head positions, meaning that it is essential to be able to accurately superimpose images.

This study employed rotation, tilt, flexion, and extension as ways to alter the head position, based on a previous study.^{1,3} After establishing the normal position, the following alterations were made: 5° of leftward rotation, 5° of leftward tilting, 5° of flexion, and 5° of extension. Changes in the head position of more than 10° were considered improbable in clinical situations, and for this reason, 5° increments were used. Instead of the well-known length and angle measurements, this study assessed differences in the landmark coordinates obtained using different head positions. In clinical settings, it is common to compare and analyze images using reference points. In order to closely imitate this workflow, the pre-reorientation image comparisons were made using the reference points obtained directly from the CBCT apparatus. These reference points were automatically set as the antero-inferior point of the FOV.

Statistically significant differences were found between the coordinates in the normal-position images and the coordinates in the varied-position images, although these differences were not of identical magnitude in the X, Y, and Z coordinates. This may have been due to the fact that some coordinates are difficult to identify in three-dimensional images, and the error resulting from that difficulty may have negated the variability due to changes in the head position. Additionally, three-dimensional changes in coordinates may not be equally distributed among the X, Y, and Z axes. The rotated and tilted positions were obtained through leftward movement, meaning that the

right-side coordinates were further from the normal-position landmarks than the left-side coordinates. Additionally, this study investigated differences between the normal-position images and the varied-position images with reorientations performed by hand to determine whether doing so would reduce error. The correction process used 3 landmarks fixed with gutta percha as reference points for axial reconstruction.

After reorientation, no statistically significant differences were found between the normal-position coordinates and the varied-position coordinates or in the distances between the coordinates. This shows that reorientation with reproducible reference points allows relatively accurate superimpositions. Lagravere et al.¹⁶ stated that small errors in marking reference points can alter the imaging results immensely. In addition, Hwang et al.¹⁸ demonstrated that small errors in marking reference points can result in overestimating the distances among coordinates. This study was able to minimize reorientation errors by replacing unreliable anatomical landmarks with reliable gutta percha indicators. By using 3 simple gutta percha marks as reference points, the reorientation process used in analyzing the pre-treatment and post-treatment three-dimensional images may be expected to become fast and easy. Even if CBCT scans are taken with different head positions, these CBCT images can be used with adequate reorientation.

In conclusion, changes in the head position led to changes in the three-dimensional image coordinates. However, the reoriented images were accurately superimposable when 3 reference points made using gutta percha were used.

References

1. El-Beialy AR, Fayed MS, El-Bialy AM, Mostafa YA. Accuracy and reliability of cone-beam computed tomography measurements: influence of head orientation. *Am J Orthod Dentofacial Orthop* 2011; 140: 157-65.
2. Kau C, Richmond S, Palomo J, Hans M. Three-dimensional cone beam computerized tomography in orthodontics. *J Orthod* 2005; 32: 282-93.
3. Sheikhi M, Ghorbanizadeh S, Abdinian M, Goroochi H, Badrihan H. Accuracy of linear measurements of Galileos cone beam computed tomography in normal and different head positions. *Int J Dent* 2012; 2012: 214954.
4. van Steenberghe D, Naert I, Andersson M, Brajnovic I, Van Cleynenbreugel J, Suetens P. A custom template and definitive prosthesis allowing immediate implant loading in the maxilla: a clinical report. *Int J Oral Maxillofac Implants* 2002; 17: 663-70.
5. Gahleitner A, Watzek G, Imhof H. Dental CT: imaging technique, anatomy, and pathologic conditions of the jaws. *Eur Radiol* 2003; 13: 366-76.
6. Cohnen M, Kemper J, Möbes O, Pawelzik J, Mödder U. Radiation dose in dental radiology. *Eur Radiol* 2002; 12: 634-7.
7. Hein E, Rogalla P, Klingebiel R, Hamm B. Low-dose CT of the paranasal sinuses with eye lens protection: effect on image quality and radiation dose. *Eur Radiol* 2002; 12: 1693-6.
8. Hagtvedt T, Aaløkken TM, Nøtthellen J, Kolbenstvedt A. A new low-dose CT examination compared with standard-dose CT in the diagnosis of acute sinusitis. *Eur Radiol* 2003; 13: 976-80.
9. Mah JK, Danforth RA, Bumann A, Hatcher D. Radiation absorbed in maxillofacial imaging with a new dental computed tomography device. *Oral Surg Oral Med Oral Pathol Oral Radiol Endod* 2003; 96: 508-13.
10. Ludlow JB, Davies-Ludlow LE, Brooks SL. Dosimetry of two extraoral direct digital imaging devices: NewTom cone beam CT and Orthophos Plus DS panoramic unit. *Dentomaxillofac Radiol* 2003; 32: 229-34.
11. Sukovic P. Cone beam computed tomography in craniofacial imaging. *Orthod Craniofac Res* 2003; 6 Suppl 1: 31-6.
12. Hashimoto K, Arai Y, Iwai K, Araki M, Kawashima S, Terakado M. A comparison of a new limited cone beam computed tomography machine for dental use with a multidetector row helical CT machine. *Oral Surg Oral Med Oral Pathol Oral Radiol Endod* 2003; 95: 371-7.
13. Ziegler CM, Woertche R, Brief J, Hassfeld S. Clinical indications for digital volume tomography in oral and maxillofacial surgery. *Dentomaxillofac Radiol* 2002; 31: 126-30.
14. Hassan B, van der Stelt P, Sanderink G. Accuracy of three-dimensional measurements obtained from cone beam computed tomography surface-rendered images for cephalometric analysis: influence of patient scanning position. *Eur J Orthod* 2009; 31: 129-34.
15. Togashi K, Kitaura H, Yonetsu K, Yoshida N, Nakamura T. Three-dimensional cephalometry using helical computer tomography: measurement error caused by head inclination. *Angle Orthod* 2002; 72: 513-20.
16. Lagravere MO, Major PW, Carey J. Sensitivity analysis for plane orientation in three-dimensional cephalometric analysis based on superimposition of serial cone beam computed tomography images. *Dentomaxillofac Radiol* 2010; 39: 400-8.
17. Kitaura H, Yonetsu K, Kitamori H, Kobayashi K, Nakamura T. Standardization of 3-D CT measurements for length and angles by matrix transformation in the 3-D coordinate system. *Cleft Palate Craniofac J* 2000; 37: 349-56.
18. Hwang JJ, Kim KD, Park H, Park CS, Jeong HG. Factors influencing superimposition error of 3D cephalometric landmarks by plane orientation method using 4 reference points: 4 point superimposition error regression model. *PLoS One* 2014; 9: e110665.
19. Sabban H, Mahdian M, Dhingra A, Lurie AG, Tadinada A. Evaluation of linear measurements of implant sites based on head orientation during acquisition: an ex vivo study using cone-beam computed tomography. *Imaging Sci Dent* 2015; 45: 73-80.
20. de Oliveira AE, Cevidanes LH, Phillips C, Motta A, Burke B, Tyndall D. Observer reliability of three-dimensional cepha-

- lometric landmark identification on cone-beam computerized tomography. *Oral Surg Oral Med Oral Pathol Oral Radiol Endod* 2009; 107: 256-65.
21. Berco M, Rigali PH Jr, Miner RM, DeLuca S, Anderson NK, Will LA. Accuracy and reliability of linear cephalometric measurements from cone-beam computed tomography scans of a dry human skull. *Am J Orthod Dentofacial Orthop* 2009; 136: 17.e1-9.
 22. Ludlow JB, Gubler M, Cevidanes L, Mol A. Precision of cephalometric landmark identification: cone-beam computed tomography vs conventional cephalometric views. *Am J Orthod Dentofacial Orthop* 2009; 136: 312.e1-10.